Experiences with Dynamical Mode Decomposition for Wide-Area Mode Estimation

Marcelo de Castro, Luigi Vanfretti
Rensselaer Polytechnic Institute
Troy, NY, USA
Email: decasm3@rpi.edu

Chetan Mishra, Xin Xu, Kevin D. Jones
Dominion Energy
Richmond, VA, USA

***Abstract*—This paper presents the authors' experience in using the Dynamical Mode Decomposition (DMD) for estimating electromechanical oscillation modes from real synchrophasor data from the Dominion Energy system. To gain insight into the effectiveness of this approach, the results obtained from DMD on ambient data are compared against frequency domain approaches. Furthermore, the challenges in using this method are highlighted. The comparison shows that DMD is suitable for mode estimation from ambient data and should be further investigated for real world deployment within wide-area monitoring systems.**

I. Introduction

Synchrophasor measurement technology was proposed in the early 1980s [1] and since then many different applications for power system monitoring have been envisioned. During the last decade, Phasor Measurement Units (PMUs) became a broadly adopted technology in the United States thanks to the "American Recovery and Reinvestment Act of 2009" which sponsored a large number of PMU installations [2] that are now producing a great amount of data with rich information that can be used for different applications [3]. The increased availability of real-time streamed measurement data support on-going transformation of power systems into Cyber-Physical Systems (CPS), where the observed measurements can be properly analyzed, and automated control strategies can be implemented [4].

Among the many applications that use PMU data and that create the basis for a power system to be transformed into a CPS, the study [5] and monitoring [6] of power system oscillations are one of the most important. In addition, electromechanical oscillations are now frequently analyzed in power systems, with wide-area modes being of particular interest [7]. Oscillations are characterized by their frequency and damping, and can be constantly monitored in order to find critical values [8], which might indicate the "stress" of the system [9]. Now, since the system is mostly in ambient conditions, [9], for online tracking of stability, mode estimation techniques applicable to such data are more attractive. In addition to the frequency and damping of oscillations, it is also very important to estimate mode shapes [3], [10] since these give insights into the observability of each mode which is useful in control applications. That being said, there are a myriad of techniques available for performing such analysis [11].

Dynamic Mode Decomposition (DMD) [12], [13] is one such approach that has recently gained traction for data driven analysis of fluid dynamics, which are governed by nonlinear PDEs. This technique is fairly efficient when dealing with large number of measurements with a small number of governing modes/dynamic patterns, and thus, offers an attractive option for data driven stability analysis of large scale power systems. This is a result of an inherent compression step using singular value decomposition (SVD) that extracts a lower dimensional subspace with significant energy. This is performed in an integrated manner with identification of temporal patterns/modes. Another attractive quality of this technique is that it has been extended to the analysis of nonlinear systems using the Koopman framework [14]. The idea behind this approach is to embed the original nonlinear system into a much higher dimensional linear system using carefully chosen observable functions. As a result, these approaches have drawn attention from the power system community. For instance, Koopman nonlinear modes were applied in [15] for the identification of coherent oscillations in machines from a power system and for data-driven power system stability assessment, respectively. In addition, [16] proposes a DMD-based algorithm for performing data-driven modal analysis of coherent electromechanical oscillations in the power system. While providing a great potential, there hasn't been much evidence on the effectiveness of DMD when used with real-world ambient synchrophasor data, specifically in comparison to the traditional frequency domain approaches. Furthermore, there is a need to understand the implications of the amount of compression chosen in DMD on the final estimated spectrum. Hence, this paper addresses this research gap.

This paper is organized as follows: Section II summarizes the DMD technique and how it can be used in modal analysis. Section III presents the case study conducted using DMD and other existing methods, while Section IV discusses obtained results. Finally, Section V draws the final conclusions of this paper.

II. Dynamical Mode Decomposition

A. Modal Analysis

Under ambient conditions, a power system will undergo small perturbations around its equilibrium $\mathbf{x_0}$ and input $\mathbf{u_0}$, and can be represented by the following linear model [17]:

$$\boldsymbol{\Delta}\dot{\mathbf{x}} = \mathbf{A}\boldsymbol{\Delta}\mathbf{x} + \mathbf{B}\boldsymbol{\Delta}\mathbf{u}. \tag{1}$$

where $\boldsymbol{\Delta}\mathbf{x}$ is the $n \times 1$ state vector, $\boldsymbol{\Delta}\mathbf{u}$ is the $r \times 1$ input vector, $\mathbf{A}$ is the $n \times n$ state matrix and $\mathbf{B}$ is the $n \times r$ input matrix. The superscript $\dot{}$ indicates the 1st-order derivative of each state with respect to time t.

The modes of oscillation are directly related to the eigenvalues of the state matrix. Stable oscillatory modes are given by a complex eigenvalue pair $\lambda_i = \sigma_i \pm j\omega_i$, where σ_i is a negative real number. The mode would have its frequency and damping given by

$$f = \frac{\omega}{2\pi}\,\text{Hz, and } \xi = \frac{-\sigma}{\sqrt{\sigma^2 + \omega^2}} \tag{2}$$

By determining the eigenvectors of the state matrix it follows that

$$\mathbf{A}\varphi_\mathbf{i} = \lambda_i\varphi_\mathbf{i}, \text{ and } \psi_\mathbf{i}\mathbf{A} = \psi_\mathbf{i}\lambda_i, \tag{3}$$

where $\varphi_\mathbf{i}$ and $\psi_\mathbf{i}$ are the right- and left-eigenvectors related to the eigenvalue λ_i. From here, each diagonal state z_i and its derivatives are given by

$$z_i = \psi_\mathbf{i}\mathbf{x}, \text{ and } \dot{z}_i = \lambda_i z_i + \psi_\mathbf{i}\mathbf{B}\mathbf{u}. \tag{4}$$

Finally, the state vector $\mathbf{x}$ can be composed as a sum of the diagonal states z_i, scaled by the right-eigenvectors $\varphi_\mathbf{i}$, that is

$$\mathbf{x} = \sum_{i=1}^{n} z_i\varphi_\mathbf{i}. \tag{5}$$

Note that (5) shows the participation of each mode in the composition of each state of $\mathbf{x}$. The right-eigenvector $\varphi_\mathbf{i}$ shows how the dynamic behavior due to λ_i impacts each state variable x_i in state vector $\mathbf{x}$. Because the elements of $\varphi_\mathbf{i}$ are complex values, both their magnitude and phase reveal the relation between the mode of oscillation and the state. Consequently, $\varphi_\mathbf{i}$ is called the mode shape of mode λ_i [3].

B. Traditional DMD

The Dynamical Mode Decomposition (DMD) [12] is a pure data-driven technique that aims at identifying the best linear model that fits the measurement data [18]. When compared to *de facto* techniques, i.e. Yule-Walker (YW), DMD-based solutions, which are well suited for multi-channel approaches, offer the advantage of allowing dynamical modes and mode-shapes to be found by eigen-decomposition of the identified model [18]. For simplicity, let us assume that $\mathbf{x}_j \in \mathbb{R}^{n\times 1}$ denotes the state vector value at time $(j-1)\Delta t$ where Δt is the sampling time step. Sampled values in columns to build data matrices

$$\mathbf{X}_k = \begin{bmatrix}\mathbf{x}_1 & \mathbf{x}_2 & \dots & \mathbf{x}_N\end{bmatrix}, \quad \text{and}$$
$$\mathbf{X}_{k+1} = \begin{bmatrix}\mathbf{x}_2 & \mathbf{x}_3 & \dots & \mathbf{x}_{N+1}\end{bmatrix}.$$

Now, a typical discrete time linear time invariant system can be represented by,

$$\mathbf{X}_{k+1} = \mathbf{A}\mathbf{X}_k. \tag{6}$$

Where $\mathbf{A}$ is the state matrix to be estimated using the standard DMD, which is briefly discussed here. For more details, please refer to [12], [13], [18]. DMD starts by calculating the rank r approximation of $\mathbf{X}_k$ using Singular Value Decomposition,

$$\mathbf{X}_k = \mathbf{U}\boldsymbol{\Sigma}\mathbf{V}^*, \tag{7}$$

where $\mathbf{U}$ is $n\times r$, $\boldsymbol{\Sigma}$ is a diagonal $r\times r$ matrix and $\mathbf{V}$ is $N\times r$ and * stands for the conjugate transpose. This is substituted in the previous equation. Pre-multiplying with $\mathbf{U}^*$ results in the following reduced order system,

$$\tilde{\mathbf{X}}_{k+1} = \mathbf{U}^*\mathbf{X}_{k+1} = \mathbf{U}^*\mathbf{A}\mathbf{U}\boldsymbol{\Sigma}\mathbf{V}^* = \tilde{\mathbf{A}}\tilde{\mathbf{X}}_k \tag{8}$$

The reduced order state matrix $\tilde{\mathbf{A}}$, which contains the dominant eigen values of $\mathbf{A}$, can easily be estimated as,

$$\tilde{\mathbf{A}} = \mathbf{U}^*\mathbf{X}_{k+1}\mathbf{V}\boldsymbol{\Sigma}^{-1}. \tag{9}$$

The right eigenvalues and eigenvectors of $\tilde{\mathbf{A}}$ can be calculated using

$$\tilde{\mathbf{A}}\mathbf{w} = \tilde{\lambda}\mathbf{w}. \tag{10}$$

Finally, the DMD mode shape corresponding to the eigenvalue $\tilde{\lambda}$ can then be calculated as

$$\hat{\varphi} = \mathbf{U}\mathbf{w}. \tag{11}$$

Note that vector $\hat{\varphi}$ is the projection of the actual mode-shape φ onto the range of $\mathbf{X}_k$ [13]. Nevertheless, the vector $\hat{\varphi}$ can be used as the mode shape of the oscillatory DMD mode denoted by $\tilde{\lambda}$. It is also important to note that $\tilde{\lambda}_i$ are eigenvalues of the discrete time linear system [8].

C. High Order DMD

The practical implementation of DMD, however, may face challenges under scarce number of available measurements and lack of observability of measurements at specific locations. To address these issues, an extension of the DMD method called Higher Order DMD (HODMD) that is based on time-lagged measurements is proposed in [19]. This method has been shown to produce better results than Auto-Regressive-Moving-Average-based (ARMA-based) methods when there is no prior knowledge of the modes' frequencies and damping rates [20]. Let us denote the measurement outputs by $\mathbf{y} \in \mathbb{R}^{m\times 1}$. This method embeds the output space $\mathbf{y}$ into a higher dimensional space using time delays. Therefore, if s time-delays are considered, the state vector value at j^{th} time step denoted by $\mathbf{x}_j$ can be written as

$$\mathbf{x}_j = \left[\mathbf{y}_j \;\; \mathbf{y}_{j-1} \dots \mathbf{y}_{j-s}\right]^\intercal. \tag{12}$$

The entire procedure from the previous section is repeated and the eigenvalues and eigenvectors are obtained. The mode shape in this case will be given by the first m values of $\tilde{\varphi}$.

Note that that two parameters need to be set in the HODMD method: the number of time-delays being embedded in the measurements and the reduced rank of the SVD. DMD-based techniques achieves compression through SVD, which characterizes dynamics based on their energy content, thereby

preferring the dominant ones. Moreover, owing to the fact that HODMD uses time redundancy through time delays, it avoids ill-conditioned data matrices formations that could result in many spurious modes [20]. Due to these interesting features the HODMD is an adequate technique that is applied for all DMD-based output-only mode estimations performed in this paper.

III. Case Study

In this study, synchronized measurement data is collected from nine PMU locations installed in different substations located throughout Dominion Energy's transmission system. Substations are made anonymous, as they are referred to as substations A, B, ..., I. The ambient data displayed in the figures of this paper comes from local frequency measurements collected at 8PM of July 23rd of 2019, lasting for 30 minutes. In order to introduce robustness to this study, a Monte Carlo approach is adopted and frequency measurements from 100 random days are also collected in order to produce the comparison between single-channel YW and Multi-Channel HODMD in the next section. The data set was collected with a sampling frequency of 30 Hz, and it was pre-processed through filtering to remove frequencies lower than 0.1 Hz and higher than 0.5 Hz. After that, the data was re-sampled at a rate of 1 Hz [21]. A sample of the pre-processed data collected from substations A, B and C is displayed in Figure 1.

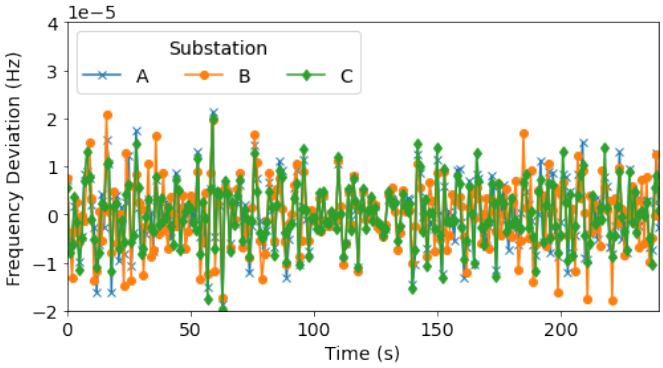

Fig. 1. Four-minute sample of pre-processed frequency signal.

Welch's method is applied to the pre-processed data in order to obtain an estimate of the Power Spectrum Density (PSD) [9], [22]. The estimate was obtained by calculating FFTs using the number of points equivalent to two minutes of data and using 50 percent overlap between data windows. The PSD estimate for all measurements is shown in Figure 2. Three dominant modes are shown to be present in all data streams and, thus, they are highlighted. The first mode is highlighted in green and it is about 0.13 Hz, the second one is in blue and its apex occurs at about 0.19 Hz, the third one is in red and has its peak at about 0.34 Hz. Note that some data streams might have other peaks appearing throughout the spectrum, just like substation E's data appear to peak at around 0.42 Hz. However, these modes are not considered to be of interest because the goal of this study is to study wide-area modes, which should be observed in every single data stream analyzed.

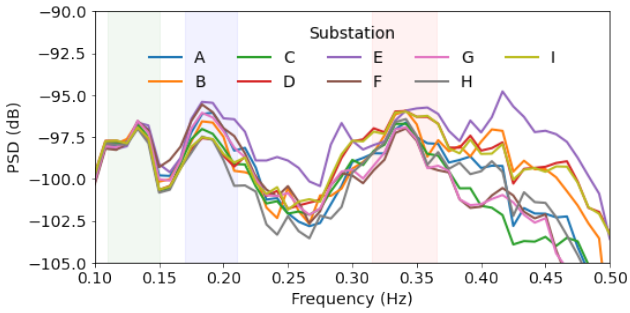

Fig. 2. Welch power spectrum density estimate for frequency data from all substations.

The modes reported here are similar to the ones observed in [5] with the exception of the first mode, which has not been reported in earlier literature. The main reason behind that is that the observability of that mode is high for this particular data set, while it might be lower in the signals studied in [5]. In addition, it is also possible that the filtering options adopted in [5] are more aggressive than the ones adopted in the current paper. In this study, the authors have selected only measurement sets that present an adequate observability level of the modes of interest.

IV. Mode and Mode-Shape Estimation

A. Single Channel HODMD

Using the data from Substation A, it is possible to obtain an estimate of the PSD [9], [22] using the Welch approach. The periodogram was built using data points corresponding to ten minutes of data and 50 percent window overlap. The PSD estimate was then used to refine the YW model order [9]. Differing from YW technique, the HODMD has two parameters to be set. The first parameter is the number of time-delays that are going to be embedded in the measurements. The second parameter is the rank of the SVD matrices. These two parameters are expected to change the number of modes and their characteristics which are identified by the technique. In order to illustrate this effect, three small tests are conducted. In each test, different parameter configuration are used for the HODMD and the results are compared with Welch estimate and the 8th order YW model.

In the first test, different time delays are embedded in the data coming from Substation A. Values of 6, 8 and 10 time delays are used and the SVD has always full rank. It means that SVD will have rank n for n time delays. The comparison between the estimates is shown in Figure 3. Note that the HODMD model with 8 time delays has many similarities with the 8th order YW model.

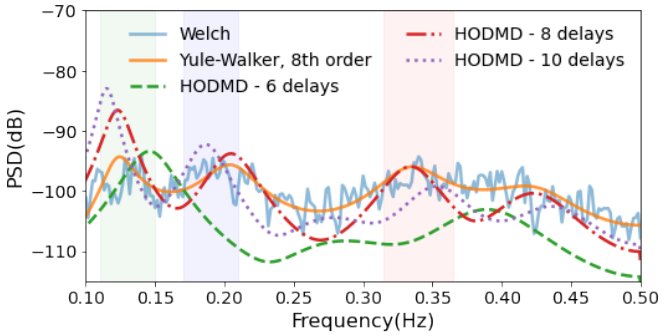

Fig. 3. Comparison between Welch power spectrum density estimate, YW model and HODMD with different number of time delays and SVD with full rank.

In the second experiment, different time delays are embedded in the data coming from Substation A but the rank of the SVD is forced to be 6 in all of them. Values of 10, 14 and 18 time delays are used. The results, which are depicted in Figure 4, show that the HODMD models with highest number of time delays find three modes. However, it is clear that a higher number of delays results in a sharpest peak, which might hinder damping estimates. This effect can be explained by the fact that an increase in the embedded time delays would result in the convergence of the estimated modes to a uniform distribution on the unit circle [23], meaning that estimation converges to pure oscillations and explaining the sharper peaks seen in Fig. 4.

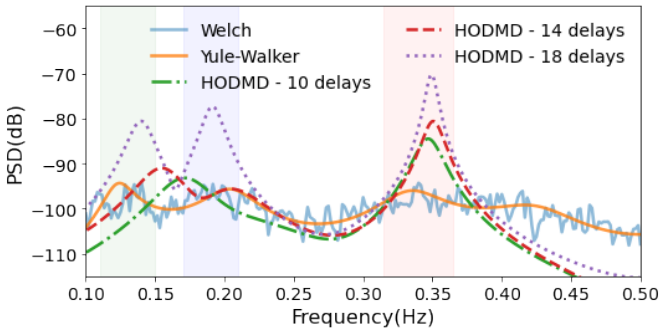

Fig. 4. Comparison between Welch power spectrum density estimate, YW model and HODMD with different number of time delays and SVD with rank 6.

Finally, in the last experiment, 10 time delays are embedded in the data coming from Substation A but the rank of the SVD is set to be 6, 8 and 10. The comparison between the models is displayed in Figure 5. Note that the rank of the SVD directly affects the number of peaks presented in the model, just like the order of YW models.

B. Multi-Channel HODMD

The HODMD is studied in the last section using a single measurement data. However, the technique is better suited for multi-channel approaches. Indeed, the HODMD technique is used in this section to estimate the frequency and damping coming from the modes that might be present in all of the measurements. The HODMD model was set to have 7 time

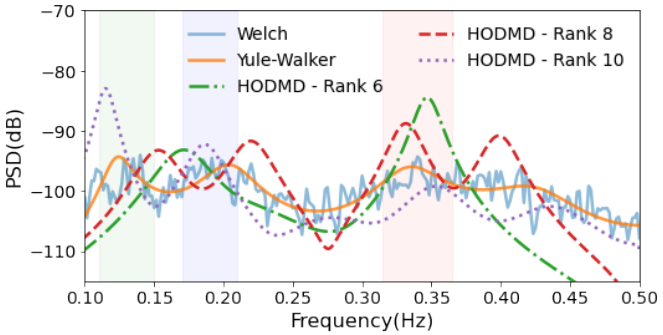

Fig. 5. Comparison between Welch power spectrum density estimate, YW model and HODMD with 10 time delays and different SVD ranks.

delays and the SVD matrices are reduced to have their rank equal to 22. The PSD estimate coming from that configuration is compared with the Welch PSD estimates from the measurements in Figure 6.

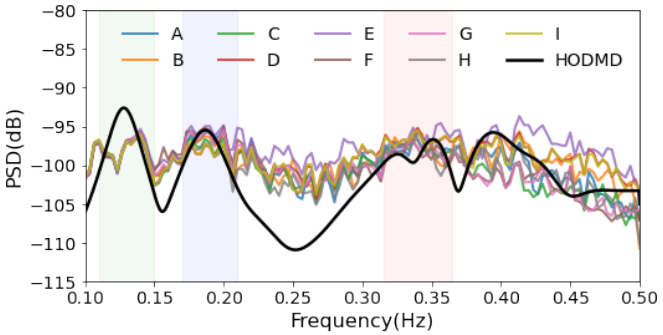

Fig. 6. Comparison between Welch power spectrum density estimates and the HODMD.

In order to create a robust estimate of the the mode's frequency and damping, the HODMD and YW techniques are applied in 100 different measurement sets, randomly collected throughout the years of 2019, 2020 and 2021. The damping and frequency bias and standard deviation estimates from both approaches are shown in Table I. Note that the modes have quite similar frequency and their damping estimates also agree, but also recall that YW is used in a single stream from the set, while HODMD is applied in all measurements from each stream set. It is interesting to note that, although the HODMD produces frequency estimates with higher variance, they are being estimated from multiple signals at once.

TABLE I
FREQUENCY AND DAMPING ESTIMATES VIA MONTE-CARLO APPROACH.

Single-Channel YW		**Multi-Channel HODMD**	
Freq. (mHz)	Damp. (%)	Freq. (mHz)	Damp. (%)
124.0 ± 1.8	7.9292 ± 1.0642	127.6 ± 2.0	9.0499 ± 1.0303
213.4 ± 3.5	11.019 ± 1.154	205.3 ± 10.5	10.291 ± 1.301
324.6 ± 5.8	9.1884 ± 1.3187	306.7 ± 17.3	9.6422 ± 1.5544

C. Mode Shape Estimation

Now, in order to estimate the mode-shape from each one of the modes, the method presented in [3] is applied. In it, the Cross-Spectral Density (CSD) calculation is crucial for the estimate of the angles between each vector. On the other hand, in DMD-based approaches, the mode shape is directly estimated from the eigenvector. In addition, for estimating the mode shape angles correctly, the method in [3] requires, as an input, the frequency of the mode. Therefore, in order to produce a better comparison between the mode shape estimates, the frequency used to calculate the mode shape via the method present in [3] was the one estimated by the HODMD procedure.

The mode shape estimates for each method is presented in Figures 7, 8, 9 for frequency bias of 0.1276, 0.2053 and 0.3067 Hz, respectively. Note that all Figures depict a similar behavior, showing that all generators studied are coherent with respect to both modes. In addition, note that as the estimated mode's frequency grows, the mode-shape diverges. This is due to the fact that the higher frequency modes have an increased damping rate and more variability, resulting in the increasing disparities between estimated mode shapes that is observed when comparing both methods in Figures 8 and 9, for example.

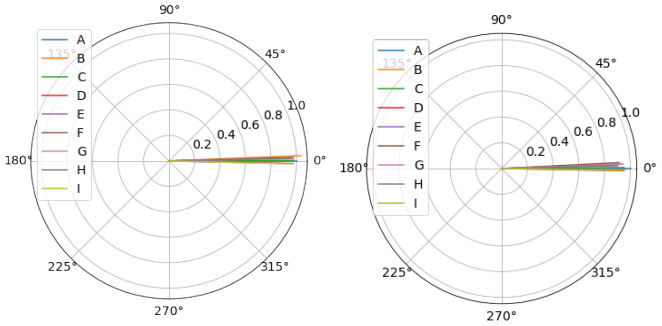

(a) CSD-based (b) DMD-based

Fig. 7. Mode shape estimate for bias of $f = 0.1276$ Hz.

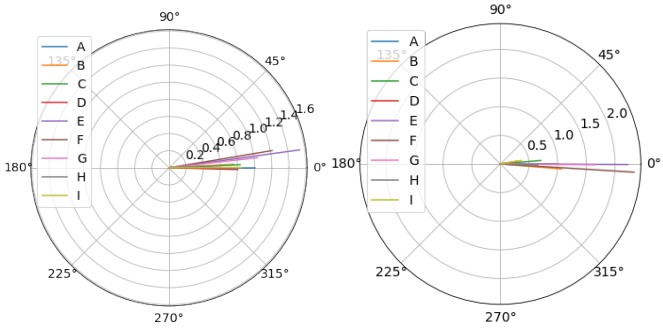

(a) CSD-based (b) DMD-based

Fig. 8. Mode shape estimate for bias of $f = 0.2053$ Hz.

V. Conclusions and Future Work

This paper presented a brief description of DMD-based approaches for power systems applications and used the techniques to study low-frequency electromechanical oscillations.

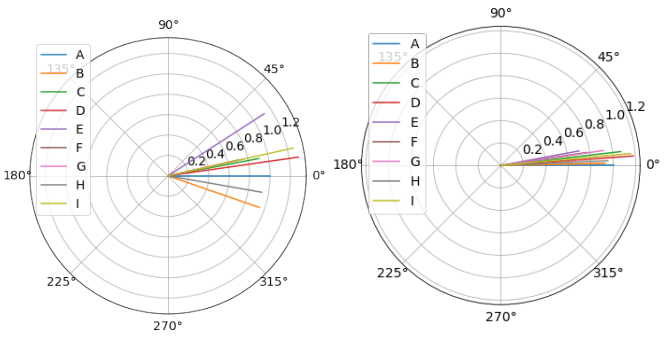

(a) CSD-based (b) DMD-based

Fig. 9. Mode shape estimate for bias of $f = 0.3067$ Hz.

Comparisons made with different parameter settings on an HODMD model show that altering the number of time delays might change the identified modes' characteristics. Moreover, the SVD rank might be tuned to find a particular number of modes, similarly to the YW model order. Results obtained with HODMD technique are compared with the YW approach and they show that both methods result on similar estimations of mode frequency and damping.

However, the DMD-based technique also allows for mode-shapes to be estimated without applying an additional procedure, which can be seen as an advantage over *de facto* techniques. Indeed, this paper presented the mode shape estimation using DMD and drew a comparison with the mode shape estimated by a CSD-based method. The results obtained from the mode shape estimation are, also, very promising, since mode shape estimates present similar behavior in both estimates. On top of that, it is necessary to highlight that the HODMD-based method is quite simple and computationally inexpensive.

The DMD-based technique presented in this paper shows good potential and, therefore, more experiments and research should be done. For instance, the authors also aim to study cases where data sets have missing measurements and how to derive data-driven models from measurement sets. Hence, this current study should be seen as a starting point on using DMD-based techniques for studying oscillations in the power system.

References

[1] A. G. Phadke, J. S. Thorpe and M. G. Adamiak, "A New measurement technique for tracking voltage phasors, local system frequency, and rate of change of frequency", *IEEE Transactions on Power Apparatus and Systems*, vol. PAS-102, No. 5, May, pp. 1025-1038, 1983.

[2] "Advancement of Synchrophasor Technology," U.S. Department of Energy, Office of Electricity Delivery and Energy Reliability , Mar-2016. [Accessed: 4-Nov-2020]

[3] D. J. Trudnowski, "Estimating electromechanical mode shape from synchrophasor measurements", *IEEE Transactions on Power Systems*, vol. 23, No. 3, August, pp. 1188-1195, 2008.

[4] E. A. Lee, "Cyber physical systems: Design challenges", In Proc. 2008 11th IEEE international symposium on object and component-oriented real-time distributed computing (ISORC), 2008, pp. 363–369.

[5] "Interconnection Reliability Analysis," North American Electric Reliability Corporation, July 2019. [Accessed: 4-Nov-2020]

[6] "Reliability Guideline: Forced Oscillation Monitoring & Mitigation," North American Reliability Corporation, September 2017. [Accessed: 4-Nov-2020]

[7] J. F. Hauer, D. J. Trudnowski and J. G. DeStesse, "A perspective on WAMS analysis tools for tracking of oscillatory dynamics", In Proc. 2007 IEEE Power Engineering Society General Meeting, 2007.

[8] V. S. Peric, X. Bombois and L. Vanfretti, "Optimal signal selection for power system ambient mode estimation using a prediction error criterion", *IEEE Transactions on Power Systems*, vol. 31, No. 4, July, pp. 2621-2633, 2016.

[9] L. Vanfretti et al., "Estimation of Eastern Denmark's Electromechanical Modes from Ambient Phasor Measurement Data", In Proc. 2010 IEEE Power Engineering Society General Meeting, 2010.

[10] L. Vanfretti et al., "Application of ambient analysis techniques for the estimation of electromechanical oscillations from measured PMU data in four diffrent power systems", *European Transactions on Electrical Power*, vol. 21, No. 4, May, pp. 1640-1656, 2011.

[11] J. J. Sanchez-Gasca and J. H. Chow, "Performance comparison of three identification methods for the analysis of electromechanical oscillations", *IEEE Transactions on Power Systems*, vol. 14, No. 3, August, pp. 995-1002, 1999.

[12] P. J. Schmid, "Dynamic mode decomposition of numerical and experimental data", *Journal of fluid mechanics*, vol. 656, August, pp. 5-28, 2010.

[13] J. H. Tu et al., "On dynamic mode decomposition: Theory and applications", *Journal of Computational Dynamics*, vol. 1, no. 2, pp. 391-421, 2014.

[14] M. O. Williams, I. G. Kevrekidis and C. W. Rowley. "A data-driven approximation of the koopman operator: extending dynamic mode decomposition",*Journal of Nonlinear Science*, vol 25, No. 6, December, pp. 1307-1346, 2015.

[15] Y. Susuki and I. Mezic, "Nonlinear Koopman modes and coherency identification of coupled swing dynamics", *IEEE Transactions on Power Systems*, vol. 26, No. 4, November, pp. 1894-1904, 2011.

[16] E. Barocio, B. C. Pal, N. F. Thornhill and A. R. Messina, "A dynamic mode decomposition framework for global power system oscillation analysis", *IEEE Transactions on Power Systems*, vol. 30, No. 6, December, pp. 2902-2912, 2014.

[17] P. Kundur, N. J. Balu and M. G. Lauby, Eds., *Power System Stability and Control*. New York: McGraw-Hill, 1994.

[18] K. Taira, S. L. Brunton, S. T. Dawson, C. W. Rowley, T. Colonius, B. J. McKeon, O. T. Schmidt, S. Gordeyev, V. Theofilis. L. S. Ukeiley, "Modal analysis on fluids: An overview", *AIAA Journal*, vol. 55, No. 12, December, pp. 4013-4041, 2017.

[19] S. Le Clainche and J. M. Vega, "Higher order dynamic mode decomposition", *SIAM Journal on Applied Dynamical Systems*, vol. 16, No. 2, pp. 882-925, 2017.

[20] C. Mendez, S. Le Clainche, R. Moreno-Ramos, J. M. Vega, "A new automatic, very efficient method for the analysis of flight flutter testing data",*Aerospace Science and Technology*, vol. 114, pp.1-15, 2021.

[21] L. Vanfretti, S. Bengtsson, J. O. Gjerde, "Preprocessing synchronized phasor measurement data for spectral analysis of electromechanical oscillations in the Nordic Grid", *International Transactions on Electrical Energy Systems*, vol. 25, No. 2, February, pp. 348-358, 2015.

[22] J. Proakis and D. Manolakis *Digital Signal Processing: Principles, Algorithms and Applications*, 4th ed., New Jersey: Prentic Hall, 2006.

[23] A. Onatski and H. Uhlig, "Unit roots in white noise", *Econometric Theory*, vol. 28, no. 3, pp. 485–508, 2012.